

## Implications of the dependence of the elastic properties of DNA on nucleotide sequence

BY WILMA K. OLSON<sup>1</sup>, DAVID SWIGON<sup>1</sup> AND BERNARD D. COLEMAN<sup>2</sup>

<sup>1</sup>*Department of Chemistry and Chemical Biology,  
Rutgers, The State University of New Jersey,  
610 Taylor Road, Piscataway, NJ 08854-8087, USA  
(olson@rutchem.rutgers.edu; swigon@jove.rutgers.edu)*

<sup>2</sup>*Department of Mechanics and Materials Science,  
Rutgers, The State University of New Jersey,  
98 Brett Road, Piscataway, NJ 08854-8058, USA  
(bcoleman@jove.rutgers.edu)*

*Published online 5 May 2004*

Recent advances in structural biochemistry have provided evidence that not only the geometric properties but also the elastic moduli of duplex DNA are strongly dependent on nucleotide sequence in a way that is not accounted for by classical rod models of the Kirchhoff type. A theory of sequence-dependent DNA elasticity is employed here to calculate the dependence of the equilibrium configurations of circular DNA on the binding of ligands that can induce changes in intrinsic twist at a single base-pair step. Calculations are presented of the influence on configurations of the assumed values and distribution along the DNA of intrinsic roll and twist and a modulus coupling roll to twist. Among the results obtained are the following. For minicircles formed from intrinsically straight DNA, the distribution of roll–twist coupling strongly affects the dependence of the total elastic energy  $\Psi$  on the amount  $\alpha$  of imposed untwisting, and that dependence can be far from quadratic. (In fact, for a periodic distribution of roll–twist coupling with a period equal to the intrinsic helical repeat length,  $\Psi$  can be essentially independent of  $\alpha$  for  $-90^\circ < \alpha < 90^\circ$ .) When the minicircle is homogeneous and without roll–twist coupling, but with uniform positive intrinsic roll, the point at which  $\Psi$  attains its minimum value shifts towards negative values of  $\alpha$ . It is remarked that there are cases in which one can relate graphs of  $\Psi$  versus  $\alpha$  to the ‘effective values’ of bending and twisting moduli and helical repeat length obtained from measurements of equilibrium distributions of topoisomers and probabilities of ring closure. For a minicircle formed from DNA that has an ‘S’ shape when stress-free, the graphs of  $\Psi$  versus  $\alpha$  have maxima at  $\alpha = 0$ . As the binding of a twisting agent to such a minicircle results in a net decrease in  $\Psi$ , the affinity of the twisting agent for binding to the minicircle is greater than its affinity for binding to unconstrained DNA with the same sequence.

**Keywords:** DNA elasticity; base-pair steps; twist-bend coupling

---

One contribution of 16 to a Theme ‘The mechanics of DNA’.

## 1. Introduction

The DNA double helix resembles a deformable rod that has a contour length of  $N \times 3.4 \text{ \AA}$ , with  $N$  the number of base pairs (bp), or, equivalently, the number of nucleotides in each of the two DNA strands. In continuum models, the familiar B form of DNA is often assigned a (steric) cross-sectional diameter of  $20 \text{ \AA}$  and a bending modulus that corresponds to a persistence length of approximately 150 bp (i.e.  $510 \text{ \AA}$ ).

Although there are cases in which one can treat a DNA molecule as a homogeneous elastic rod that is straight when stress free and has uniform elastic properties, high-resolution structural studies show that the geometrical properties of DNA are sequence dependent with each base-pair step, i.e. set of two neighbouring base-pairs, tending to adopt a three-dimensional structure that depends on the nucleotide composition of the step. Both the intrinsic structure and elastic properties, which are characterized by the functions describing the energetics of relative rotation and displacement of neighbouring base pairs, depend on sequence. Some base-pair steps act as natural wedges that change the direction of the helical axis; others are sites of under- or overtwisting relative to the average twist of *ca.*  $36^\circ$ . The local bends, if appropriately grouped in phase with the (*ca.* 10 bp per full turn) double helical structure, can give the DNA intrinsic curvature (Trifonov 1991; Crothers *et al.* 1992; Hagerman 1992). Bending anisotropy can occur if local stiffness is appropriately in phase with the helical repeat (Matsumoto & Olson 2002).

There is evidence that the six motions of relative rotation and displacement of neighbouring base pairs depicted in figure 1*a* can be strongly coupled (Olson *et al.* 1998). The untwisting of adjacent residues induces an increase in roll, the parameter that describes the component of bending with predominant influence on the widths of the major and minor grooves. Untwisting also induces a decrease in slide, the parameter describing motion of a base-pair plane along its major axis of inertia.†

We recently formulated a theory of a general class of DNA models in which the total elastic energy  $\Psi$  is the sum of the interaction energies of adjacent base pairs. In that theory (Coleman *et al.* 2003) the energy  $\psi^n$  assigned to the  $n$ th base-pair step is taken to be given by a function  $\tilde{\psi}^n$  of the six kinematical variables that specify the orientation and displacement of the  $n$ th and  $(n + 1)$ th base pairs. These variables, also called base-pair step parameters, are two components of bending, *tilt*  $\theta_1$  and *roll*  $\theta_2$ , a measure of *twist*  $\theta_3$ , two components of shear (here the shear is a relative motion of the base-pairs in a step and not a deformation of a single base pair), *shift*  $\rho_1$  and *slide*  $\rho_2$ , and a measure of extension called *rise*  $\rho_3$ .‡ (Schematic representations of these base-pair step parameters are given in figure 1.) In the cited paper it is shown that the complementarity of DNA bases, the antiparallel alignment of the two DNA

† The duplex forms of DNA differ in their average values of the intrinsic kinematical variables. For example, the helical repeat length is *ca.* 11 bp for the A form, *ca.* 10 bp for the B form, *ca.* 9 bp for the C form and *ca.* 8 bp for the D form. The intrinsic values of the twist, roll, and slide as one goes from one of these forms to another show correlations analogous to the couplings described in the text for deformations of B DNA. Specifically, the average intrinsic roll decreases and slide increases as one goes from A to B to C to D DNA (Lu & Olson 2003).

‡ The *rise* of a base-pair step corresponds to the characteristic *ca.*  $3.4 \text{ \AA}$  separation of closely stacked aromatic rings, and is not necessarily equivalent to the length of the line connecting the centres of neighbouring base pairs or the projection of that line on the double-helical axis.

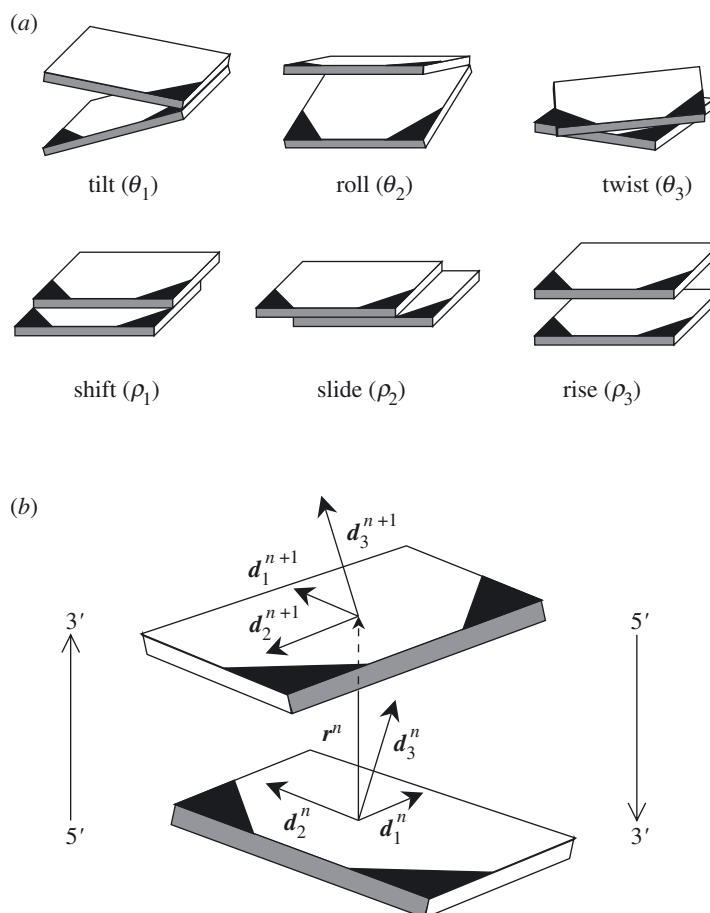


Figure 1. (a) Schematic of parameters describing the relative orientation and displacement of successive base pairs. *Tilt* and *roll* measure local bending, *twist* measures rotation in the base-pair plane, *shift* and *slide* local shearing, and *rise* local stretch. For precise definitions see equations (2.3)–(2.5). (b) A base-pair step showing the vectors  $\mathbf{r}^n$ ,  $\mathbf{d}_j^n$ ,  $\mathbf{d}_j^{n+1}$ . Each nucleotide is covalently bonded (at its darkened corner) to one of the two sugar–phosphate chains. The arrows give the 5′–3′ directions of those chains. Shaded edges lie in the minor groove of DNA.

strands, and the requirement that the  $\psi^n$  be invariant under a change in the choice of the strand for which the 5′–3′ direction is parallel to the direction of increasing  $n$ , place restrictions on the functions  $\tilde{\psi}^n$ . The theory gives rise to variational equations of equilibrium that can be written as equations of balance of moments and forces.

In the broad class of models covered by the theory, the simplest one compatible with the experimental data presently available employs the assumption that  $\tilde{\psi}^n$  is, for each  $n$ , a quadratic function of the differences  $\Delta\theta_1$ ,  $\Delta\theta_2$ ,  $\Delta\theta_3$ ,  $\Delta\rho_1$ ,  $\Delta\rho_2$ ,  $\Delta\rho_3$  between the present values of the variables  $\theta_1$ ,  $\theta_2$ ,  $\theta_3$ ,  $\rho_1$ ,  $\rho_2$ ,  $\rho_3$  and their intrinsic (i.e. stress-free) values  $\bar{\theta}_1$ ,  $\bar{\theta}_2$ ,  $\bar{\theta}_3$ ,  $\bar{\rho}_1$ ,  $\bar{\rho}_2$ ,  $\bar{\rho}_3$ . For that model, which accounts for coupling between changes in these variables by allowing the constitutive functions  $\tilde{\psi}^n$  to contain cross-terms, we developed an efficient  $O(N)$  method (with  $N$  the number of base pairs) for calculating solutions of the equations of equilibrium and determining

their stability.† In the same paper we reported calculations of the effect of bound untwisting ligands on configurations and elastic energies for a 150 bp DNA minicircle made up of two types of base-pair steps arranged in such a way that the molecule has a nearly circular stress-free configuration and hence can be termed a ‘DNA o-ring’. The DNA was rendered effectively inextensible and unsharable by taking the elastic moduli corresponding to shift, slide and rise to be large. These calculations extended earlier studies indicating that the response of an o-ring to untwisting is markedly different from that of a minicircle of intrinsically straight DNA.‡ We found that the configuration and elastic energy of a DNA o-ring depend strongly on the spatial distribution of intercalated untwisting agents, and that the presence in  $\tilde{\psi}^n$  of cross-terms that couple roll to twist not only introduces an asymmetry in the configurational response of the macromolecule to local untwisting, but, in appropriate circumstances, leads to the occurrence of a first-order transition between two distinct stable equilibrium configurations with equal elastic energy and equal amounts of the imposed untwisting.

In this paper we consider DNA minicircles formed from sequences of three types of base-pair steps: (1) steps (called i steps) for which the intrinsic values  $\bar{\theta}_1$  and  $\bar{\theta}_2$  of the tilt and roll are both zero, and the matrix of elastic moduli contains no cross-terms coupling kinematical variables; (2) steps (called c steps) with  $\bar{\theta}_1 = \bar{\theta}_2 = 0$  but with a non-zero value of the modulus  $F_{23}$  coupling roll and twist; and (3) steps with intrinsic roll, i.e.  $\bar{\theta}_1 = 0$  and  $\bar{\theta}_2 > 0$ , but no coupling (called r and r\* steps, depending on the assumed values of  $\bar{\theta}_2$  and  $\bar{\theta}_3$ ). We calculate the minimum energy configurations of such minicircles, assuming that they have been untwisted by a positive or negative amount  $\alpha$  at a single base-pair step. We find that the elastic energy  $\Psi$  of minicircles formed from intrinsically straight DNA is remarkably sensitive to the way in which the roll–twist coupling modulus  $F_{23}$  is distributed along the DNA molecule. For an appropriate distribution of  $F_{23}$ , the calculated departure of  $\Psi$  from quadratic dependence on  $\alpha$  can be so large that  $\Psi$  is essentially independent of  $\alpha$  for  $-90^\circ < \alpha < 90^\circ$ .

If a minicircle is homogeneous and without roll–twist coupling, but with uniform non-zero intrinsic roll  $\bar{\theta}_2$ , then, because of the helical nature of DNA, the bends occurring in the two halves of each helical repeat length, being of equal magnitudes but in opposite directions, cancel each other. In contrast with the even dependence of  $\Psi$  on  $\alpha$  (i.e.  $\Psi(\alpha) = \Psi(-\alpha)$ ) shown by minicircles with  $\bar{\theta}_2 = 0$ , we find that as  $\bar{\theta}_2$  increases through positive values the calculated graph of  $\Psi$  versus  $\alpha$  becomes skewed, and the point at which  $\Psi$  attains its minimum shifts toward negative values of  $\alpha$ . Finally, we observe that the calculated minimum energy configurations of minicircles formed from DNA that has an S-shape in its stress-free configuration depend upon the site of imposed untwisting. This dependence is such that, for each  $\alpha$ ,  $\Psi$  is minimized when the twisting agent is bound to a region with zero intrinsic curvature. In addition, although the location of the binding site has an influence on the occurrence of minima of  $\Psi(\alpha)$  and the values of  $\alpha$  at which they are attained,  $\Psi(\alpha)$  has its maximum value at  $\alpha = 0$ . Thus, the binding of a twisting agent to a minicircle formed

† In the present theory a configuration is said to be stable if it gives a local minimum to  $\Psi$  in the class of all configurations obeying the imposed constraints.

‡ See, for example, Bauer *et al.* (1993), White *et al.* (1996), Charitat & Fourcade (1998) and other papers cited by Coleman *et al.* (2003).

from intrinsically S-shaped DNA leads to a decrease in  $\Psi$  and hence is energetically more favourable than the binding of the same agent to a segment of unconstrained (i.e. not circularized) DNA with the same base-pair sequence.

## 2. Constitutive relations and variational equations

In the present theory base pairs are represented by rectangular objects and the configuration of a DNA segment with  $N + 1$  base pairs (and hence  $N$  base-pair steps) is specified by giving, for  $1 \leq n \leq N + 1$ , both the location  $\mathbf{x}^n$  of the centre of the rectangle  $\mathcal{B}^n$  that represents the  $n$ th base pair and a right-handed orthonormal triad  $\mathbf{d}_1^n, \mathbf{d}_2^n, \mathbf{d}_3^n$  that is embedded in the base pair as shown in figure 1b.† The *axial curve* of the segment is the polygonal curve  $\mathcal{C}$  comprised of the  $N$  line segments connecting the spatial points  $\mathbf{x}^1, \dots, \mathbf{x}^{N+1}$ .

We take the elastic energy  $\Psi$  of a configuration to be the sum over  $n$  of the energy  $\psi^n$  of interaction of the  $n$ th and  $(n + 1)$ th base pairs, i.e.

$$\Psi = \sum_{n=1}^N \psi^n. \quad (2.1)$$

Here  $\psi^n$ , the elastic energy of the  $n$ th step, is a function of the relative orientation and displacement of the  $(n + 1)$ th base pair with respect to the  $n$ th base pair or, equivalently, of the components of the vectors  $\mathbf{d}_j^{n+1}$  and  $\mathbf{r}^n = \mathbf{x}^{n+1} - \mathbf{x}^n$  with respect to the basis  $\mathbf{d}_i^n$ . As the  $3 \times 3$  matrix with entries  $D_{ij}^n = \mathbf{d}_i^n \cdot \mathbf{d}_j^{n+1}$  is orthogonal, it can be parametrized by a triplet  $(\theta_1^n, \theta_2^n, \theta_3^n)$  of angles, with  $\theta_1^n$  the *tilt*,  $\theta_2^n$  the *roll* and  $\theta_3^n$  the *twist* of  $\mathcal{B}^{n+1}$  relative to  $\mathcal{B}^n$ . The displacement variables  $\rho_1^n, \rho_2^n, \rho_3^n$ , called *shift*, *slide* and *rise* (see figure 1a) are related to the numbers  $\mathbf{r}_i^n = \mathbf{d}_i^n \cdot \mathbf{r}^n$  by a coordinate transformation of the type  $\rho_i^n = \hat{\rho}_i(\theta_1^n, \theta_2^n, \theta_3^n, r_1^n, r_2^n, r_3^n)$ , in which the functions  $\hat{\rho}_i$ , whose form is independent of  $n$ , are determined by equations (2.3)–(2.5). The elastic energy  $\psi^n$  of the  $n$ th base-pair step is given by a constitutive relation of the form

$$\psi^n = \tilde{\psi}^n(\theta_1^n, \theta_2^n, \theta_3^n, \rho_1^n, \rho_2^n, \rho_3^n), \quad (2.2)$$

in which the function  $\tilde{\psi}^n$  depends on the nucleotide composition of the  $n$ th and  $(n + 1)$ th base pairs.

The definition of the kinematical variables  $\theta_i^n$  and  $\rho_i^n$  employed here follows a procedure, introduced by Zhurkin *et al.* (1979) and further developed by El Hassan & Calladine (1995), in which one employs the Euler-angle system  $\zeta^n, \kappa^n, \eta^n$  for which

$$D_{ij}^n = \mathbf{d}_i^n \cdot \mathbf{d}_j^{n+1} = Z_{ik}(\zeta^n) Y_{kl}(\kappa^n) Z_{lj}(\eta^n), \quad (2.3a)$$

$$[Y_{ij}(\alpha)] = \begin{bmatrix} \cos \alpha & 0 & \sin \alpha \\ 0 & 1 & 0 \\ -\sin \alpha & 0 & \cos \alpha \end{bmatrix}, \quad [Z_{ij}(\alpha)] = \begin{bmatrix} \cos \alpha & -\sin \alpha & 0 \\ \sin \alpha & \cos \alpha & 0 \\ 0 & 0 & 1 \end{bmatrix}, \quad (2.3b)$$

† As seen in the figure, the vectors  $\mathbf{d}_i^n$  are defined so that  $\mathbf{d}_3^n$  is perpendicular to  $\mathcal{B}^n$  with  $\mathbf{d}_3^n \cdot \mathbf{r}^n > 0$ ;  $\mathbf{d}_2^n$  is parallel to the long edges of  $\mathcal{B}^n$  and points toward the short edge containing the corner of  $\mathcal{B}^n$  bonded to a deoxyribose moiety in the sugar–phosphate chain for which  $n$  increases in the 5′–3′ direction;  $\mathbf{d}_1^n = \mathbf{d}_2^n \times \mathbf{d}_3^n$  is parallel to the short edges of  $\mathcal{B}^n$  and points toward the major groove of the DNA. For the relation between  $\mathbf{x}^n, \mathbf{d}_1^n, \mathbf{d}_2^n, \mathbf{d}_3^n$  and the coordinates of base-pair atoms, see the discussion of Olson *et al.* (2001).

and defines  $\theta_1^n, \theta_2^n, \theta_3^n$  by the equations:

$$\zeta^n = \frac{1}{2}\theta_3^n - \gamma^n, \quad \eta^n = \frac{1}{2}\theta_3^n + \gamma^n, \quad (2.4a)$$

$$\kappa^n = \sqrt{(\theta_1^n)^2 + (\theta_2^n)^2}, \quad \tan \gamma^n = \frac{\theta_1^n}{\theta_2^n}. \quad (2.4b)$$

Following El Hassan & Calladine (1995), we here define  $\rho_i^n$  so that

$$r_i^n = \mathbf{d}_i^n \cdot \mathbf{r}^n = \bar{D}_{ij}^n \rho_j^n, \quad (2.5a)$$

$$\bar{D}_{ij}^n = \mathbf{d}_i^n \cdot \bar{\mathbf{d}}_j^n = Z_{ik}(\zeta^n) Y_{kl}(\frac{1}{2}\kappa^n) Z_{lj}(\gamma^n). \quad (2.5b)$$

Throughout this paper, as in the above equations, the subscripts  $i, j, k, l$  take the values 1, 2, 3, and the Einstein summation convention is used for repeated subscripts (but not superscripts). Equation (2.5a) implies that the  $\rho_i^n$  are the components of  $\mathbf{r}^n$  with respect to an orthonormal basis  $\bar{\mathbf{d}}_i^n$ , called the ‘mid-basis for step  $n$ ’, which is defined by (2.5b). The definitions of  $\theta_i^n$  and  $\rho_i^n$  are such that, for each configuration of the molecule, a change in the choice of the direction of increasing  $n$  leaves  $\theta_2, \theta_3, \rho_2, \rho_3$  invariant but changes the sign of  $\theta_1$  and  $\rho_1$ . A number of computer programs have been developed to reduce atomic coordinate data of the type available for DNA crystal structures in the Nucleic Acid Database (Berman *et al.* 1992) to variables, such as the six quantities  $\theta_i^n, \rho_i^n$  defined above, that are compatible with the Cambridge convention (Dickerson *et al.* 1989). For surveys see Lu *et al.* (1999) and Lu & Olson (1999).

The function  $\tilde{\psi}^n$  in (2.2) depends on the nucleotide bases that are in the  $n$ th and  $(n+1)$ th base pairs. Let us now discuss the restrictions imposed on  $\tilde{\psi}^n$  by the complementarity of A to T and G to C, the antiparallel directions of the sugar-phosphate chains, and the assumption that  $\tilde{\psi}^n$  is independent of the composition of base pairs other than the  $n$ th and  $(n+1)$ th. To do so we may write  $\tilde{\psi}^{XY}$  for  $\tilde{\psi}^n$ , where XY, with X in the  $n$ th and Y in the  $(n+1)$ th base pair, is a sequence of two nucleotide bases attached to the chain for which  $n$  increases in the 5′–3′ direction. (When this notation is employed we refer to the  $n$ th base-pair step as an ‘XY step’.) For the complement of the base X, one shall write  $\bar{X}$  (i.e.  $\bar{A} = T, \bar{G} = C$ ). The complement of a sequence of bases is the sequence of complementary bases in the reverse order: the complement of XY is  $\bar{Y}\bar{X}$  (e.g. the complement of AC is GT, because  $\bar{X}$  and  $\bar{Y}$  are attached at the locations  $n$  and  $n+1$  to the chain for which  $n$  decreases in the 5′–3′ direction.) As we have shown elsewhere (Coleman *et al.* 2003), when  $\theta_i^n, \rho_i^n$  are defined by (2.3)–(2.5), each function  $\tilde{\psi}^{XY}$  determines its complementary function  $\tilde{\psi}^{\bar{Y}\bar{X}}$  by the relation

$$\tilde{\psi}^{XY}(\theta_1^n, \theta_2^n, \theta_3^n, \rho_1^n, \rho_2^n, \rho_3^n) = \tilde{\psi}^{\bar{Y}\bar{X}}(-\theta_1^n, \theta_2^n, \theta_3^n, -\rho_1^n, \rho_2^n, \rho_3^n). \quad (2.6)$$

It follows that, if XY is self-complementary, i.e. if  $XY = \bar{Y}\bar{X}$ , then  $\tilde{\psi}^{XY}$  is an even function of the pair  $(\theta_1^n, \rho_1^n)$  for each fixed value of the quadruple  $(\theta_2^n, \theta_3^n, \rho_2^n, \rho_3^n)$ .

For the calculations presented here we take  $\psi^n$  to be a quadratic function of  $\Delta\theta_i^n = \theta_i^n - \bar{\theta}_i^n, \Delta\rho_i^n = \rho_i^n - \bar{\rho}_i^n$ , where  $\bar{\theta}_i^n$  and  $\bar{\rho}_i^n$  are the intrinsic values, i.e. values appropriate to a stress-free state. Thus,

$$\psi^n = \frac{1}{2}F_{ij}^n(\Delta\theta_i^n)(\Delta\theta_j^n) + G_{ij}^n(\Delta\theta_i^n)(\Delta\rho_j^n) + \frac{1}{2}H_{ij}^n(\Delta\rho_i^n)(\Delta\rho_j^n), \quad (2.7)$$

where  $F_{ij}^n$ ,  $G_{ij}^n$  and  $H_{ij}^n$  are constants with  $F_{ij}^n = F_{ji}^n$  and  $H_{ij}^n = H_{ji}^n$ , ( $i, j = 1, 2, 3$ ). It follows from (2.6) that if we replace  $F_{ij}^n$  by  $F_{ij}^{\text{XY}}$ , etc., and let  $\bar{Z}$  stand for  $F$ ,  $G$ , or  $H$ , then in (2.7)

$$\bar{\theta}_i^{\text{XY}} = Q_{ij} \bar{\theta}_j^{\bar{\text{YX}}}, \quad \bar{\rho}_i^{\text{XY}} = Q_{ij} \bar{\rho}_j^{\bar{\text{YX}}}, \quad Z_{ij}^{\text{XY}} = Q_{ik} Z_{kl}^{\bar{\text{YX}}} Q_{lj}, \quad (2.8)$$

where

$$Q_{ij} = 0 \quad \text{for } i \neq j, \quad -Q_{11} = Q_{22} = Q_{33} = 1. \quad (2.9)$$

Equations (2.8) imply that, when  $\text{XY} = \text{AT}, \text{GC}, \text{TA}$  or  $\text{CG}$ ,

$$F_{12}^{\text{XY}} = F_{13}^{\text{XY}} = 0, \quad H_{12}^{\text{XY}} = H_{13}^{\text{XY}} = 0, \quad (2.10 a)$$

$$G_{12}^{\text{XY}} = G_{13}^{\text{XY}} = G_{21}^{\text{XY}} = G_{31}^{\text{XY}} = 0, \quad \bar{\theta}_1^{\text{XY}} = \bar{\rho}_1^{\text{XY}} = 0. \quad (2.10 b)$$

The quadratic energy functions in (2.7), which can be regarded as first approximations to more general nonlinear functions of  $\Delta\theta_i^n$  and  $\Delta\rho_i^n$ , appear to be compatible with sequence-dependent properties of DNA deduced from the observed spatial arrangements of base pairs in high-resolution crystallographic structures. Although estimates of the intrinsic values  $\bar{\theta}_i^{\text{XY}}$  and  $\bar{\rho}_i^{\text{XY}}$  of the kinematical parameters obtained from averages of the available structural data have not changed significantly since the first reports (Gorin *et al.* 1995; Berman & Olson 2003), estimates of elastic moduli  $F_{ij}^{\text{XY}}$ ,  $G_{ij}^{\text{XY}}$  and  $H_{ij}^{\text{XY}}$  are expected to change as new structural data become available. The literature contains suggestions of correlations in DNA structure of longer range than those accounted for in the present theory in which each base pair interacts only with its nearest neighbours (such suggestions arise from interpretations of solution measurements (Nadeau & Crothers 1989; Brukner *et al.* 1995) and analysis of certain crystal structures (Packer *et al.* 2000)). There are not yet available sufficient crystallographic data to determine the dependence of elastic properties of DNA on longer-range interactions.

As we assume here that the DNA under consideration is free from external forces and moments, we define an *equilibrium configuration* to be one for which the first variation of the elastic energy  $\Psi$  vanishes for all variations in configuration that are admissible in the sense that they are compatible with the imposed constraints, in particular, those following from the assumption that the DNA molecule is a closed ring. In Coleman *et al.* (2003) we show that the resulting variational equations can be written

$$\mathbf{f}^n - \mathbf{f}^{n-1} = \mathbf{0}, \quad \mathbf{m}^n - \mathbf{m}^{n-1} = \mathbf{f}^n \times \mathbf{r}^n, \quad 2 \leq n \leq N, \quad (2.11)$$

where  $\mathbf{f}^n$  and  $\mathbf{m}^n$  are the force and moment that the  $(n+1)$ th base pair exerts on the  $n$ th base pair. The vectors  $\mathbf{f}^n$  and  $\mathbf{m}^n$  are the analogues of the vectors  $\mathbf{F}(s^*)$  and  $\mathbf{M}(s^*)$  that in Kirchhoff's theory of elastic rods (see, for example, Dill 1992; Coleman *et al.* 1993; Coleman & Swigon 2004) are interpreted as the resultant force and moment of the contact forces (i.e. Piola stresses) exerted on the cross-section with the arc length coordinate  $s^*$  by the material with arc length coordinates  $s > s^*$ . The components of  $\mathbf{f}^n$  and  $\mathbf{m}^n$  with respect to the local basis  $\mathbf{d}_i^n$  are given by

$$f_i = \frac{\partial \tilde{\psi}^n}{\partial \rho_j^n} \bar{D}_{ji}^n, \quad m_i = \Gamma_{ij}^n \left( \frac{\partial \tilde{\psi}^n}{\partial \theta_j^n} + j A_{kl}^n \rho_l^n \frac{\partial \tilde{\psi}^n}{\partial \rho_k^n} \right), \quad (2.12)$$

where  $\bar{D}_{ji}^n(\theta_1^n, \theta_2^n, \theta_3^n)$  is as in (2.3), and analytic expressions for  $\Gamma_{ij}^n$  and  ${}_jA_{kl}^n$ , which also depend on  $(\theta_1^n, \theta_2^n, \theta_3^n)$ , are given in eqns (2.13), (A1)–(A4) of Coleman *et al.* (2003).

A closed  $N$  bp segment of DNA can be considered as an  $N + 1$  bp segment that is subject to the constraint that its terminal base pairs coincide, i.e. have the same location and orientation so that

$$\mathbf{x}^1 = \mathbf{x}^{N+1}, \quad \mathbf{d}_i^1 = \mathbf{d}_i^{N+1}. \quad (2.13)$$

An equilibrium configuration is here called *stable* if it gives a strict *local* minimum to the total elastic energy  $\Psi$ . A necessary condition for an equilibrium configuration to be stable is that there be no admissible variation in configuration for which  $\delta^2\Psi$ , the second variation of  $\Psi$ , is negative. As a configuration is described in the present theory by giving a finite number of variables, namely the  $6N$  numbers,  $\theta_1^n, \theta_2^n, \theta_3^n, \rho_1^n, \rho_2^n, \rho_3^n$ , we can say that a sufficient condition for stability is that  $\delta^2\Psi$  be (strictly) positive for all admissible variations. A configuration that is stable in the present sense but does not give a global minimum to  $\Psi$  is sometimes called metastable. In practice, to verify stability we express  $\delta^2\Psi$  as a quadratic form on the  $6(N + 1)$ -dimensional space of the components (with respect to a fixed basis) of the vectors  $\delta\mathbf{x}^n$  that characterize the variation in the displacement of base pairs and the vectors  $\mathbf{w}^n$  that characterize the variation in the orientation of base pairs, i.e. the variation in the vector triads  $(\mathbf{d}_1^n, \mathbf{d}_2^n, \mathbf{d}_3^n)$  through the relation  $\delta\mathbf{d}_i^n = \mathbf{w}^n \times \mathbf{d}_i^n$  (a fuller discussion is given by Coleman *et al.* (2003)). If the smallest proper number of  $\delta^2\Psi$  is positive, the configuration under consideration is stable.

Equations (2.11), with  $\mathbf{f}^n$  and  $\mathbf{m}^n$  given by (2.12), are a system  $\mathcal{E}$  of  $6N - 6$  nonlinear algebraic equations for the unknown coordinates  $\theta_1^n, \theta_2^n, \theta_3^n, \rho_1^n, \rho_2^n, \rho_3^n$ ; that system is weakly coupled in the sense that, for each  $n$ ,  $2 \leq n \leq N$ , it is a set of six equations that can be solved numerically (using a Newton–Raphson procedure) to obtain  $(\theta_i^n, \rho_i^n)$  for given  $(\theta_i^{n-1}, \rho_i^{n-1})$ . This makes it possible to solve  $\mathcal{E}$  efficiently (using  $O(N)$  computational steps) with a recursive algorithm in which, for each  $n$ ,  $(\theta_i^n, \rho_i^n)$  is obtained as a function of  $(\theta_i^1, \rho_i^1)$ . Equilibrium configurations of segments subject to specified end conditions are calculated using an iterative scheme in which  $(\theta_i^1, \rho_i^1)$  is repeatedly adjusted until the equations (2.13) hold.

### 3. Elastic properties of the DNA studied here

Estimates of the intrinsic parameters and elastic constants of DNA derived from base-pair configurations observed in X-ray crystal structures indicate that these quantities are strongly dependent on nucleotide sequence (Olson *et al.* 1998) and have the following qualitative properties. The intrinsic tilt  $\bar{\theta}_1^{\text{XY}}$  of step XY is generally smaller than the intrinsic roll  $\bar{\theta}_2^{\text{XY}}$  for the same step, with  $\bar{\theta}_1^{\text{XY}}$  between zero and *ca.*  $1.5^\circ$ , and  $\bar{\theta}_2^{\text{XY}}$  between *ca.*  $0.5^\circ$  and *ca.*  $5^\circ$ . The intrinsic twist  $\bar{\theta}_3^{\text{XY}}$  is anticorrelated with  $\bar{\theta}_2^{\text{XY}}$ , i.e. base-pair steps with high positive values of  $\bar{\theta}_2^{\text{XY}}$  are generally underwound relative to intrinsically straight DNA (Gorin *et al.* 1995; Olson *et al.* 1998). These properties of  $\bar{\theta}_1, \bar{\theta}_2, \bar{\theta}_3$  were taken into account when we assigned values to parameters for the calculations reported here. Thus we put  $\bar{\theta}_1 = 0$  at each base-pair step and lowered  $\bar{\theta}_3$  at steps with positive intrinsic roll (table 1). When we assign a positive value to  $\bar{\theta}_2$ , that value is generally greater than that found in B-DNA crystal structures, and our choice is consistent with the value of  $\bar{\theta}_2$  associated with protein-induced



Table 1. Employed values of elastic moduli and intrinsic kinematical parameters

| step<br>type | $A$<br>( $kT \text{ deg}^{-2}$ ) | $F_{33}/A$ | $F_{23}/A$ | $\bar{\theta}_1$<br>(deg) | $\bar{\theta}_2$<br>(deg) | $\bar{\theta}_3$<br>(deg) | $\bar{\rho}_1$<br>(Å) | $\bar{\rho}_2$<br>(Å) | $\bar{\rho}_3$<br>(Å) |
|--------------|----------------------------------|------------|------------|---------------------------|---------------------------|---------------------------|-----------------------|-----------------------|-----------------------|
| i            | 0.0427                           | 1.4        | 0          | 0                         | 0                         | 36                        | 0                     | 0                     | 3.4                   |
| c            | 0.0427                           | 1.4        | 0.8        | 0                         | 0                         | 36                        | 0                     | 0                     | 3.4                   |
| r            | 0.0427                           | 1.4        | 0          | 0                         | 7.41                      | 35.57                     | 0                     | 0                     | 3.4                   |
| r*           | 0.0427                           | 1.4        | 0          | 0                         | chosen to<br>obey (3.1)   | chosen to<br>obey (3.1)   | 0                     | 0                     | 3.4                   |

transformations of DNA from the B to the A form (Lu *et al.* 2000; Berman & Olson 2003).

The estimated elastic constants have the following properties. The ratio of the tilt modulus  $F_{11}^{\text{XY}}$  to the roll modulus  $F_{22}^{\text{XY}}$  is in the range *ca.* 1 to *ca.* 5, and the ratio of the twist modulus  $F_{33}^{\text{XY}}$  to the harmonic mean

$$A^{\text{XY}} = 2 \left[ \frac{1}{F_{11}^{\text{XY}}} + \frac{1}{F_{22}^{\text{XY}}} \right]^{-1}$$

of the tilt and roll moduli is between *ca.* 0.5 and *ca.* 1.8. The roll–twist coupling modulus  $F_{23}^{\text{XY}}$  is positive and less than *ca.*  $0.03kT \text{ deg}^{-2}$ . For simplicity, we here assume that DNA bends isotropically at all base-pair steps, i.e. that  $F_{11} = F_{22} = A$ , and for each step we set  $A$  equal to  $0.0427kT \text{ deg}^{-2}$ , which corresponds to intrinsically straight DNA with a persistence length of 150 bp. We take the ratio of the twist modulus to the bending modulus to be toward the high end of observed values, i.e.  $F_{33}/F_{22} = 1.4$ , a value that is compatible with measurements of equilibrium topoisomer distributions for DNA minicircles (Horowitz & Wang 1984) and measurements of the fluorescence depolarization anisotropy of ethidium bromide molecules intercalated in DNA minicircles (Heath *et al.* 1996). For base-pair steps with the coupling modulus  $F_{23}$  not zero, we take the ratio  $F_{23}/F_{22}$  to be 0.8, which corresponds to the strong coupling of roll and twist observed in the crystallographic data for AA, AC and AT base-pair steps (Olson *et al.* 1998). We assume throughout that the moduli  $F_{13}$  and  $F_{12}$  coupling tilt to roll and twist are zero.

For simplicity, we put  $\bar{\rho}_1 = \bar{\rho}_2 = 0$ ,  $\bar{\rho}_3 = 3.4 \text{ Å}$ , and treat DNA as inextensible and unshearable by taking the moduli for shift, slide, and rise (i.e.  $H_{11}$ ,  $H_{22}$ ,  $H_{33}$ ) to be large enough to suppress changes in these variables. Hence, the calculations we present here do not take into account the known sequence-dependent variation of intrinsic slide  $\bar{\rho}_2$  and the strong coupling of slide to both roll and twist. The influence of roll, twist and slide on the macroscopic properties of supercoiled DNA will be discussed elsewhere.

The DNA minicircles treated in the present work are constructed from the four types of base-pair steps listed in table 1. A step of type i is appropriate to DNA that is intrinsically straight ( $\bar{\theta}_1 = \bar{\theta}_2 = 0$ ) and free from roll–twist coupling ( $F_{23} = 0$ ); it has elastic properties characterized by two constants, the bending and twisting moduli  $A$  and  $C$  with  $A = F_{11} = F_{22}$  and  $C = F_{33}$ , and it corresponds to the often employed ‘idealized rod model’ for DNA. A step of type c has the same stress-free configuration as an i step but has a non-zero value of  $F_{23}$ , the modulus coupling roll to twist. The steps of types r and r\* differ from an i step in that for them  $\bar{\theta}_2$  is positive

Table 2. Composition of the minicircles studied

| minicircle         | composition         | description   |
|--------------------|---------------------|---|
| I                  | $i_{150}$           | intrinsically straight homogeneous DNA with no coupling                                     |
| $I_{\text{per}}^c$ | $(i_5c_5)_{15}$     | intrinsically straight DNA with periodically distributed roll–twist coupling                |
| $I_{\text{sym}}^c$ | $((i_5c_5)_7i_5)_2$ | intrinsically straight DNA with symmetrically distributed roll–twist coupling               |
| $I_{\text{all}}^c$ | $c_{150}$           | intrinsically straight DNA with uniform roll–twist coupling                                 |
| H                  | $r_{150}^*$         | DNA with uniform positive intrinsic roll and reduced intrinsic twist obeying equation (3.1) |
| S                  | $((i_5r_5)_7i_5)_2$ | intrinsically curved DNA with no coupling   |
| $S^c$              | $((c_5r_5)_7c_5)_2$ | intrinsically curved DNA with roll–twist coupling in each intrinsically straight subsegment |
| O                  | $(i_5r_5)_{15}$     | DNA o-ring, i.e. DNA with a circular stress-free configuration, with no coupling            |

and  $\bar{\theta}_3$  has a value reduced to below  $36^\circ$ . For  $r$  steps,  $\bar{\theta}_2 = 7.41^\circ$  and  $\bar{\theta}_3 = 35.57^\circ$ ; these values are such that a 150 bp segment composed of 15 subsegments of length 10 bp, in which the first five steps are of type  $i$  and the last five are of type  $r$ , is stress-free when closed into a minicircle. (Such a minicircle is labelled ‘O’ and discussed below.)

For steps of type  $r^*$ , the parameters  $\bar{\theta}_2$  and  $\bar{\theta}_3$  are chosen in accord with the relation (see Lu & Olson 2003)

$$2 \cos \omega = \cos \bar{\theta}_3 (1 + \cos \kappa) - (1 - \cos \kappa), \quad \kappa = \sqrt{(\bar{\theta}_1)^2 + (\bar{\theta}_2)^2}. \quad (3.1)$$

We consider three examples of such steps; these are obtained by putting  $\omega = 36^\circ$ ,  $\bar{\theta}_1 = 0$ ,  $\bar{\theta}_2 = 5^\circ, 10^\circ$  or  $15^\circ$  and using (3.1) to obtain a value of  $\bar{\theta}_3$  (i.e.  $\bar{\theta}_3 = 35.66^\circ, 34.63^\circ$  or  $32.82^\circ$ , respectively). These steps are employed to construct three homogeneous (i.e. spatially uniform) minicircles labelled  $H_\alpha, H_\beta, H_\gamma$ . The number  $\omega$ , called the *helical twist*, can be defined as follows. In a base-pair step (say the  $n$ th), the orthogonal transformation that takes the basis  $\mathbf{d}_i^n$  into the basis  $\mathbf{d}_i^{n+1}$  is determined when one gives an axis of rotation and an angle of rotation;  $\omega$  is that angle. When the intrinsic parameters are independent of  $n$ , the *helical repeat length* (in bp units) is  $\Lambda = 360^\circ/\omega$ .

The composition of a minicircle is specified by giving a sequence of its base-pair steps; a subscript indicates the number of repetitions of a step, e.g.  $i_5$ , or the number of repetitions of a sequence of steps, e.g.  $(c_5r_5)_7$ . As we here confine attention to cases in which  $i, c$  and  $r$  steps are repeated five times, we call  $i_5$  an ‘ $i$  unit’,  $c_5$  a ‘ $c$  unit’, and  $r_5$  an ‘ $r$  unit’. An example is the sequence appropriate to what we shall later refer to as minicircle  $I_{\text{sym}}^c$ :

$$\begin{aligned} I_{\text{sym}}^c : ((i_5c_5)_7i_5)_2 &= (i_5c_5)_7i_5(i_5c_5)_7i_5 \\ &= i_5c_5i_5c_5i_5c_5i_5c_5i_5c_5i_5c_5i_5c_5i_5c_5i_5c_5i_5c_5i_5c_5i_5c_5i_5c_5i_5i_5; \end{aligned}$$

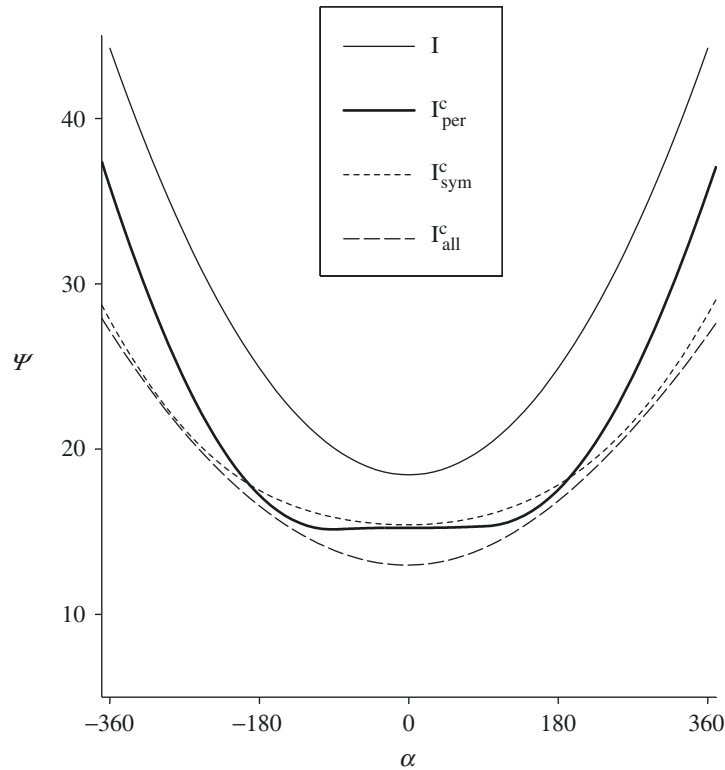


Figure 2. Calculated total elastic energy  $\Psi$  as a function of the reduction  $\alpha$  of intrinsic twist imposed at the base-pair step for which  $n = 1$ . The graphs shown are for minimum energy configurations of minicircles of intrinsically straight DNA with patterns of roll–twist coupling described in table 2. Here and in figures 4 and 5,  $\Psi$  is in  $kT$  and  $\alpha$  in degrees. Each of those figures contains, for comparison, the graph of  $\Psi$  versus  $\alpha$  for minicircle I.

this sequence has two identical halves, each made up of a total of eight i units and seven c units. We consider eight basic types of 150 bp minicircles formed from i, c, r and  $r^*$  units. The various minicircles are described in table 2.

#### 4. Results

We have now assembled the apparatus needed to present the results of our calculations of the dependence of elastic energies of the globally stable configurations of the minicircles on the amount  $\alpha$  of reduction in intrinsic twist imposed at a single base-pair step. Our calculations were designed to mimic the effect of a protein or small molecule that locally unwinds or overwinds DNA at its binding site.

##### (a) Minicircles of intrinsically straight DNA

The minicircles I,  $I_{\text{per}}^c$ ,  $I_{\text{sym}}^c$ ,  $I_{\text{all}}^c$  are made up of intrinsically straight DNA and differ from each other in the number and distribution of base-pair steps with roll–twist coupling. Although minicircle I contains only i units and minicircle  $I_{\text{all}}^c$  only c units,  $I_{\text{per}}^c$  and  $I_{\text{sym}}^c$  contain both i and c units. In  $I_{\text{per}}^c$  there are 15 units of each

type, i and c, placed in alternation to form the periodic structure  $(i_5c_5)_{15}$ . In  $I_{\text{sym}}^c$  there are 16 i units and 14 c units, joined to form the sequence  $((i_5c_5)_{7i_5})_2$ , which upon closure yields a minicircle with a single axis of flip symmetry. (We use the term flip symmetry in the sense proposed by Domokos (1995) and employed by Domokos & Healey (2001).) Figure 2 contains graphs of the calculated dependence of the minimum elastic energy  $\Psi$  on the reduction  $\alpha$  in intrinsic twist at the first base-pair step ( $n = 1$ ). We find that for each of these minicircles the shape of the axial curve  $\mathcal{C}$  stays close to a circle as  $\alpha$  varies over a range greater than that for which we present data ( $-360^\circ < \alpha < 360^\circ$ ), and  $\Psi$  is a convex function of  $\alpha$  with its minimum at  $\alpha = 0$  (figure 2). Thus, despite the presence of localized coupling,  $I_{\text{per}}^c$ ,  $I_{\text{sym}}^c$  and  $I_{\text{all}}^c$  have a behaviour similar to that of a minicircle formed from an ‘ideal elastic rod’, i.e. a homogeneous, intrinsically straight rod obeying the theory of Kirchhoff with two elastic constants,  $A$  and  $C$ .<sup>†</sup>

As expected, in the case of minicircle I, which contains only i steps,  $\Psi$  as a function of  $\alpha$  is not only convex but also quadratic. When roll–twist coupling is present, as is the case for  $I_{\text{per}}^c$ ,  $I_{\text{sym}}^c$  and  $I_{\text{all}}^c$ , the elastic energy  $\Psi$  is, for each  $\alpha$ , smaller than the corresponding value for minicircle I, and the dependence of  $\Psi$  on  $\alpha$  shows departures from quadratic behaviour. When data on equilibrium topoisomer distributions of minicircles (often called miniplasmids) and relative rates of cyclization and dimerization (from ring closure experiments) are employed to obtain information about elastic properties of DNA (see, for example, Horowitz & Wang 1984; Crothers *et al.* 1992), it is commonly assumed that the DNA under investigation is ideal, with bending and twisting moduli  $A$  and  $C$  and helical repeat length  $\Lambda$ . (As mentioned above, in the present naturally discrete theory the analogue of such a rod is a DNA molecule which, like minicircle I, contains only i steps.) The values of  $A$ ,  $C$  and  $\Lambda$  that one can calculate from measured topoisomer distribution and ring closure data under the assumption of intrinsic uniformity, namely the assumption that the parameters  $\bar{\theta}_i^n$  and  $\bar{\rho}_i^n$  are independent of  $n$ , may be called ‘effective values’ and denoted by  $A^{\text{eff}}$ ,  $C^{\text{eff}}$ ,  $\Lambda^{\text{eff}}$ . If the assumption of intrinsic uniformity holds, but it is not true that each base-pair step is an i step, then  $A^{\text{eff}}$ ,  $C^{\text{eff}}$  and  $\Lambda^{\text{eff}}$  will not be equal to the true values of  $A$ ,  $C$  and  $\Lambda$ , i.e. to  $2/[(1/F_{11}) + (1/F_{22})]$ ,  $F_{33}$ , and  $360^\circ/\omega$  with  $\omega$  given by equation (3.1). When, as here, in addition to the validity of the assumption of intrinsic uniformity we know that  $\Psi$  is a convex function of  $\alpha$  with its minimum at  $\alpha = \alpha^*$  (which implies that the equilibrium distribution of topoisomers will not be bimodal),  $A^{\text{eff}}$ ,  $C^{\text{eff}}$  and  $\Lambda^{\text{eff}}$  are determined as follows by the quadratic expansion of  $\Psi(\alpha)$  about  $\alpha^*$ :

$$A^{\text{eff}} = \frac{2N}{360^2}\Psi(\alpha^*), \quad C^{\text{eff}} = \left[ N \frac{\partial^2 \Psi}{\partial \alpha^2} \right]_{\alpha=\alpha^*}, \quad \Lambda^{\text{eff}} = \frac{360N}{360Lk + \alpha^*}; \quad (4.1)$$

here  $Lk$  is the linking number of the DNA in the minicircle. For the minicircles studied in this subsection,  $\alpha^* = 0$  and  $\Lambda^{\text{eff}} = 10$  bp. For  $I_{\text{per}}^c$ ,  $I_{\text{sym}}^c$  and  $I_{\text{all}}^c$ , the value

<sup>†</sup> The minimum energy configuration of a minicircle formed from an ideal elastic rod remains circular up to a critical value of  $\alpha$  (i.e.  $\alpha^* = (A/F_{33})3^{1/2}$  turns) at which a transition to a figure-of-eight configuration occurs. Here  $F_{33}/A = 1.4$  and hence  $\alpha^* = 445^\circ$ . Coleman *et al.* (2000) have calculated configurations and bifurcation diagrams for rings formed from impenetrable, intrinsically straight, inextensible elastic rods with  $C/A = 1.5$ , which is close to the present value of  $F_{33}/A$ . See also a recent paper of Coleman & Swigon (2000) and Coleman & Swigon (2004) (in which figures are presented for cases in which  $C/A = 1.4$ ).

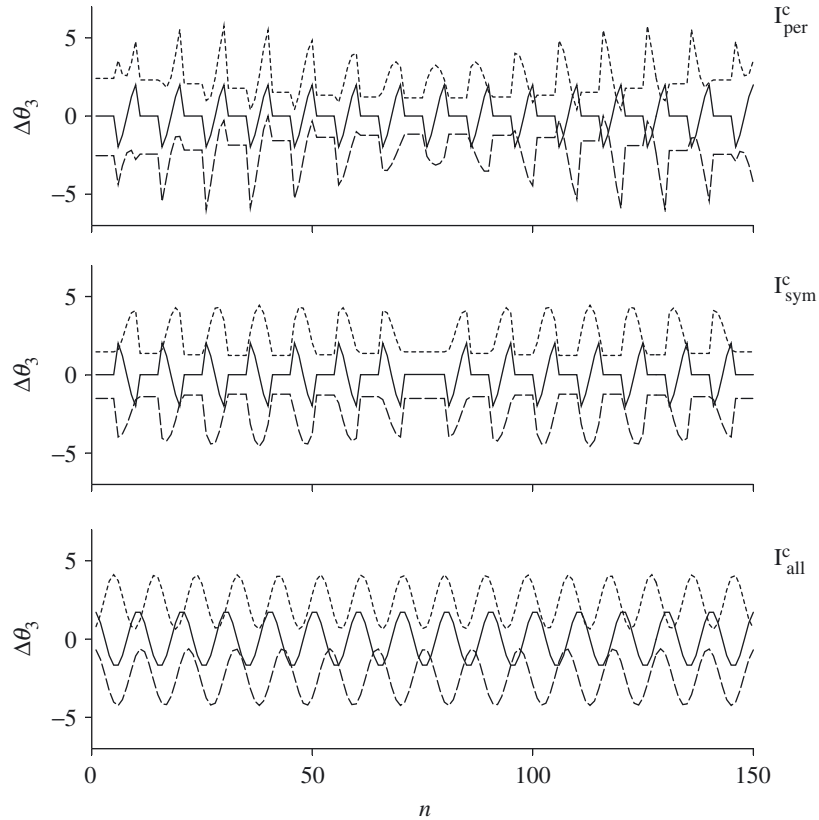


Figure 3. Excess twist  $\Delta\theta_3$ , in degrees, as a function of base-pair step  $n$  for minimum energy configurations of minicircles of figure 2 subject to the reduction  $\alpha$  of intrinsic twist imposed at the step  $n = 1$ : dashed line,  $\alpha = -360^\circ$ ; solid line,  $\alpha = 0^\circ$ ; dotted line,  $\alpha = +360^\circ$ .

of  $\Psi$  at  $\alpha = 0$ , which equals the bending energy required to close the minicircle, is lower than the value for minicircle I. In other words, the presence of coupling lowers the effective bending modulus  $A^{\text{eff}}$ . The differences

$$A^{\text{eff}}(I_{\text{per}}^c) - A^{\text{eff}}(I_{\text{all}}^c) \quad \text{and} \quad A^{\text{eff}}(I_{\text{sym}}^c) - A^{\text{eff}}(I_{\text{all}}^c)$$

are nearly identical and equal approximately one-half of the magnitude of  $A^{\text{eff}}(I_{\text{all}}^c) - A^{\text{eff}}(I)$ . Our calculations indicate that  $A^{\text{eff}}$  is approximately linear in the fraction of  $c$  steps in the minicircle.

As we see in figure 2, the elastic energy  $\Psi$  of minicircle  $I_{\text{per}}^c$  is nearly independent of  $\alpha$  for  $-90^\circ < \alpha < 90^\circ$ . This lack of resistance to changes in  $\alpha$  implies that  $C^{\text{eff}}$  is essentially zero for  $I_{\text{per}}^c$ ; in fact for that minicircle the relations (4.1) yield  $C^{\text{eff}}/A^{\text{eff}} = 0.004$ . For  $I_{\text{sym}}^c$  and  $I_{\text{all}}^c$ ,  $\Psi(\alpha)$  is not only convex, but strictly convex with  $\partial^2\Psi/\partial\alpha^2 > 0$ ;  $C^{\text{eff}}/A^{\text{eff}}$  equals 0.50 for  $I_{\text{sym}}^c$  and 1.19 for  $I_{\text{all}}^c$ . (See also table 3.) The excess twist  $\Delta\theta_3^n$  in minicircle I is independent of  $n$  for each  $\alpha$ . For the other minicircles the distribution of  $\Delta\theta_3^n$  reflects the distribution of  $c$  units (see figure 3). As expected from earlier work,  $\Delta\theta_3^n$  is uniform (i.e. independent of  $n$ ) within each  $i$  unit. The non-uniform variation of twist in  $c$  units, however, reduces the magnitude of twist in  $i$  units of minicircle  $I_{\text{sym}}^c$  compared with the values characteristic of minicircle I,

Table 3. *Effective bending and twisting moduli and effective helical parameters for minicircles studied*(In each case,  $A = 0.0427kT \text{ deg}^{-2}$ ,  $C/A = 1.4$ ,  $\Lambda = 10 \text{ bp per turn}$ .)

| minicircle                  | $A^{\text{eff}}$<br>( $kT \text{ deg}^{-2}$ ) | $C^{\text{eff}}/A^{\text{eff}}$ | $\Lambda^{\text{eff}}$<br>(bp per turn) |
|-----------------------------|---|---------------------------------|---|
| I                           | 0.0427  | 1.4                             | 10                                      |
| $I_{\text{per}}^{\text{c}}$ | 0.035   | 0.004                           | 10                                      |
| $I_{\text{sym}}^{\text{c}}$ | 0.036   | 0.50                            | 10                                      |
| $I_{\text{all}}^{\text{c}}$ | 0.030   | 1.19                            | 10                                      |
| $H_{\alpha}$                | 0.042   | 1.55                            | 10.06                                   |
| $H_{\beta}$                 | 0.041   | 1.94                            | 10.11                                   |
| $H_{\gamma}$                | 0.040   | 2.46                            | 10.15                                   |

for which  $\Delta\theta_3^n = \pm 2.4^\circ$  when  $\alpha = \pm 360^\circ$ . In minicircle  $I_{\text{all}}^{\text{c}}$  the excess twist  $\Delta\theta_3^n$  is approximately a sinusoidal function of  $n$ .

(b) *Minicircles with uniform intrinsic roll*

Each of the intrinsically homogeneous minicircles  $H_{\alpha}$ ,  $H_{\beta}$  and  $H_{\gamma}$  contains one type of  $r^*$  step and hence has  $\bar{\theta}_2$  and  $\bar{\theta}_3$  independent of  $n$  with  $\bar{\theta}_2 > 0$  and  $\bar{\theta}_3 < 36^\circ$  in accord with equation (3.1) with  $\omega = 36^\circ$ . In a stress-free state the base-pair centres of the DNA comprising such a minicircle lie not on a straight line but rather on a helical curve with radius  $R$  determined by  $\bar{\theta}_2$  and  $\bar{\theta}_3$ . However, in each case the value of  $R$  is less than  $20 \text{ \AA}$ , the assumed cross-sectional diameter of DNA, and hence the minicircle can be thought of as being close to intrinsically straight.

Figure 4 tells us that, for a minicircle composed of identical  $r^*$  steps, an increase in  $\bar{\theta}_2$  increases the skewness of the graph of  $\Psi$  versus  $\alpha$  and lowers (i.e. renders more negative) the value  $\alpha^*$  of  $\alpha$  at which  $\Psi$  attains its (unique) minimum. We find that for  $H_{\alpha}$  (which has  $\bar{\theta}_2 = 5^\circ$ ) and for  $H_{\beta}$  ( $\bar{\theta}_2 = 10^\circ$ ),  $\Psi$  is a convex function of  $\alpha$  for all  $\alpha$ . For  $H_{\gamma}$  ( $\bar{\theta}_2 = 15^\circ$ ), although  $\Psi(\alpha)$  is not convex, it is monotonically decreasing for  $\alpha < \alpha^*$  and monotonically increasing for  $\alpha > \alpha^*$ , which ensures that the equilibrium topoisomer distributions for  $H_{\gamma}$  will not be bimodal. Hence we may use equations (4.1) to calculate  $A^{\text{eff}}$ ,  $C^{\text{eff}}$  and  $\Lambda^{\text{eff}}$  for not only  $H_{\alpha}$  and  $H_{\beta}$ , but also  $H_{\gamma}$ ; results are shown in table 3. We note that  $A^{\text{eff}}$  and  $\Lambda^{\text{eff}}$  appear to vary roughly linearly with  $\bar{\theta}_2$ .

(c) *Minicircles with non-uniform intrinsic curvature*

Minicircle S contains 16 i units and 14 r units that are grouped to obtain 14 subsegments ( $i_5r_5$ ) and two i units; these subsegments and units are joined to obtain the sequence

$$S : ((i_5r_5)_7i_5)_2 = (i_5r_5)_7i_5(i_5r_5)_7i_5 \\ = \left\{ (i_5r_5) \right\} \left\{ (i_5r_5) \right\} \left\{ (i_5r_5) \right\} \left\{ (i_5r_5) \right\} (i_5r_5)(i_5r_5)(i_5r_5)i_5(i_5r_5)_7i_5.$$

The DNA of this minicircle has an intrinsic configuration that is attained only when it is cut to form an *open* segment. In figure 5a one sees the intrinsic (stress-free)

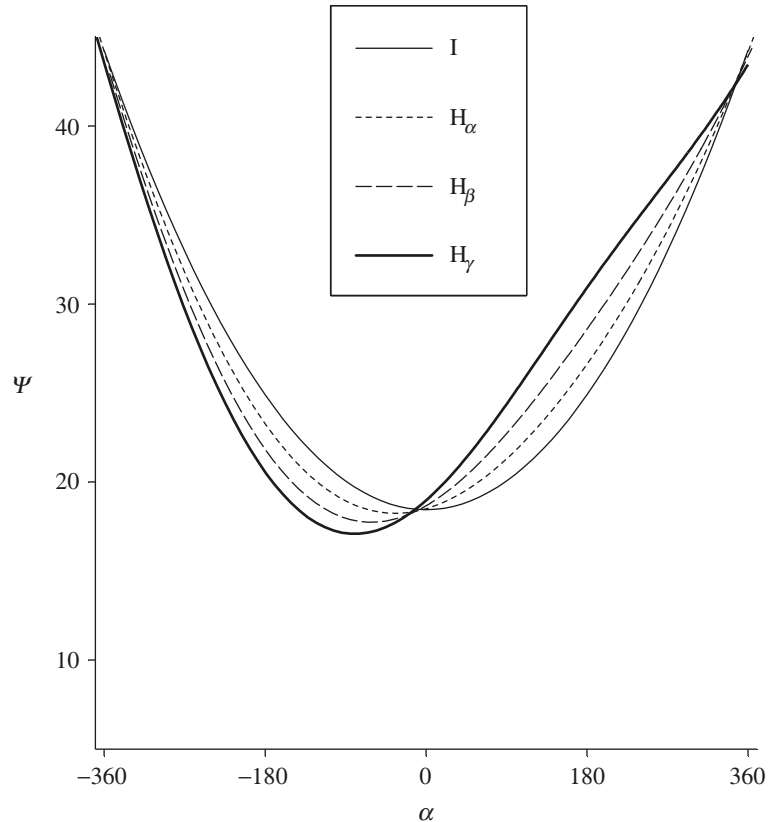


Figure 4. Calculated total elastic energy  $\Psi$  versus intrinsic twist reduction  $\alpha$  for minimum energy configurations of minicircles composed of identical steps with the following values of intrinsic roll and twist  $(\bar{\theta}_2, \bar{\theta}_3)$ :  $H_\alpha$  ( $5^\circ, 35.66^\circ$ );  $H_\beta$  ( $10^\circ, 34.63^\circ$ );  $H_\gamma$  ( $15^\circ, 32.82^\circ$ ).

configurations of the five open segments  $S_1, S_{11}, S_{21}, S_{31}, S_{41}$  obtained by cutting  $S$  at the base-pair steps with  $n = 1, 11, 21, 31, 41$ , i.e. at the sites indicated by dashed vertical lines in the sequence for  $S$ . Our notation and method of enumeration are such that the sequence of the open segment  $S_1$  is the same as that of  $S$ . The sequences of the open segments  $S_{11}, S_{21}, S_{31}, S_{41}$  are

$$\begin{aligned} S_{11} &: (i_5r_5)_6i_5(i_5r_5)_7i_5(i_5r_5), \\ S_{21} &: (i_5r_5)_5i_5(i_5r_5)_7i_5(i_5r_5)_2, \\ S_{31} &: (i_5r_5)_4i_5(i_5r_5)_7i_5(i_5r_5)_3, \\ S_{41} &: (i_5r_5)_3i_5(i_5r_5)_7i_5(i_5r_5)_4. \end{aligned}$$

We note that whereas the base-pair step of  $S$  with  $n = 1$  (i.e. the first step) is in a region of inflection for the stress-free state, i.e. a region of minimum curvature, the steps with  $n = 31$  and  $41$  are in a region where the intrinsic curvature has its maximum value. In cases such as the present in which the minicircle is not spatially uniform in its properties, the graphs of  $\Psi$  versus the amount  $\alpha$  of reduction in intrinsic twist at a single step depend on the location of that step. Such graphs are shown for minicircle  $S$  in figure 5*b*. These graphs are symmetric about  $\alpha = 0$  and, in contrast

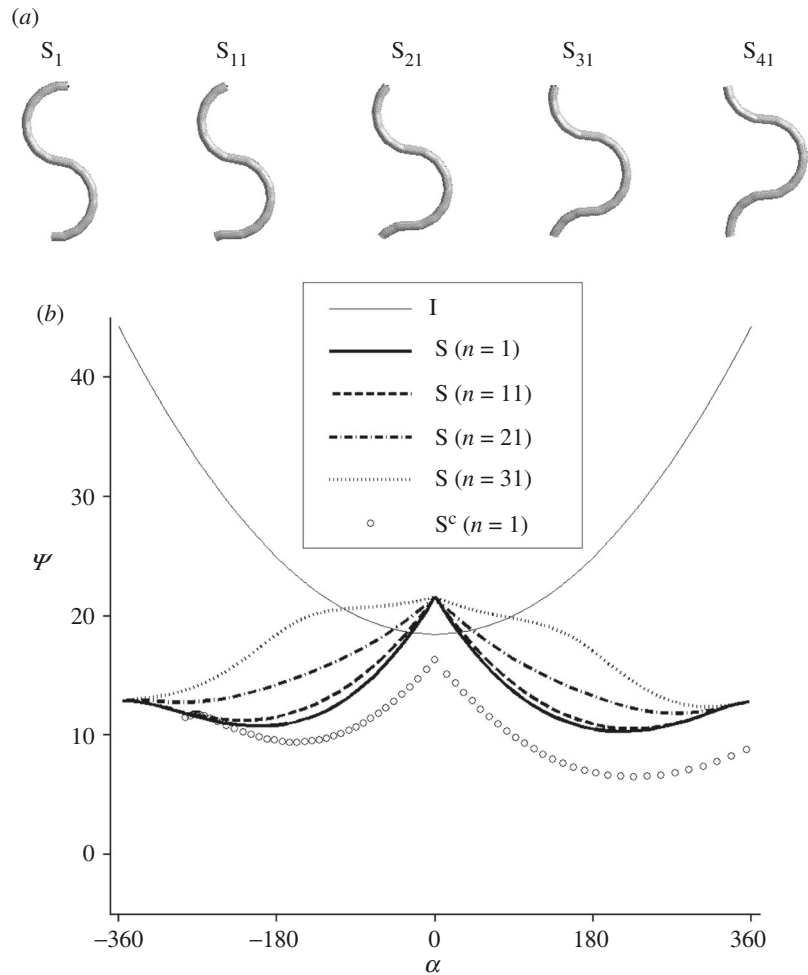


Figure 5. (a) Stress-free configurations of open segments with the sequences  $S_n$ ,  $n = 1, 11, 21, 31, 41$  that are obtained by cutting the minicircle  $S$  at the appropriate base-pair steps, as stated in the text. In each case the segment is oriented so that the  $n$ th base-pair is at the top of the drawing. (b) The total elastic energy  $\Psi$  of minicircle  $S$  as a function of the amount  $\alpha$  of reduction in intrinsic twist imposed at the  $n$ th base-pair step. Arguments based on symmetry properties of the minicircle and mechanical properties of sequences of  $i$  steps show that the graph for  $S_{41}$  is identical to that for  $S_{31}$ . Also shown is the graph of  $\Psi$  versus  $\alpha$  for untwisting of minicircle  $S^c$  at the step  $n = 1$ .

to those shown in figures 2 and 4, give  $\Psi(\alpha)$  its maximum value at  $\alpha = 0$ . When  $n = 1, 11$ , and  $21$ ,  $\Psi(\alpha)$  has two local maxima that are symmetric about  $\alpha = 0$ .<sup>†</sup>

Also shown in figure 5 is a graph of this type for the minicircle  $S^c$ , which has the base-pair sequence  $((c_5r_5)_7c_5)_2$  obtained from the sequence for  $S$  by replacing each

<sup>†</sup> This observation is not surprising and is compatible with calculations performed by Furrer *et al.* (2000) of configurations of circularized intrinsically S-shaped elastic rods and the Monte Carlo calculations of equilibrium distributions of topoisomers performed by Katritch & Vologodskii (1997) for larger plasmids with intrinsic configurations of similar shapes.



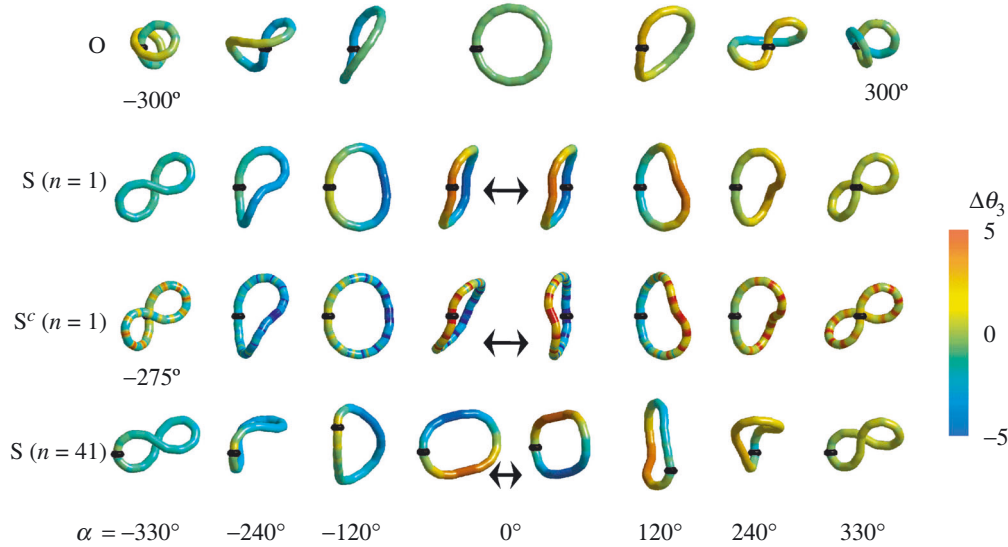


Figure 6. Selected minimum energy configurations of minicircles of intrinsically curved DNA subject to intrinsic twist reduction  $\alpha$  at the first base-pair step. The colour indicates the value of  $\Delta\theta_3$ , with blue corresponding to  $\Delta\theta_3 < 0$ , green to  $\Delta\theta_3 = 0$ , and yellow/red to  $\Delta\theta_3 > 0$  (see the colour scale). In each case the location of imposed untwisting is indicated by a black band. The compositions of the minicircles are as described in the text and in table 2. Only contact-free configurations are shown. If the minimum energy configuration of a minicircle with  $\alpha = -330^\circ$  (or  $\alpha = +330^\circ$ ) is not free from contact, the contact-free configuration with the smallest (or largest) value  $\alpha^{\min}$  (or  $\alpha^{\max}$ ) of  $\alpha$  is shown and that value is indicated. The two-sided arrows indicate that each of the minicircles S and  $S^c$  has at  $\alpha = 0$  two minimum energy configurations which are congruent but have functions  $n \rightarrow \Delta\theta_3^n$  that differ by a cyclic shift.

i unit by a c unit. As for S, for  $S^c$  the reduction in intrinsic twist is imposed at  $n = 1$ . Although it is not symmetric about  $\alpha = 0$ , that graph has its maximum there, and has two local minima.† (We note that the open segments obtained by cutting S and  $S^c$  at a given base-pair step have the same shape, i.e. the same axial curve when in their stress-free states.)

The results obtained for minicircle S show that  $\Psi(\alpha)$  is minimized for each fixed  $\alpha$  when the reduction in intrinsic twist is imposed at the step with  $n = 1$  (or the equivalent step  $n = 76$ ). This suggests that if a reduction in intrinsic twist is the result of the binding of a twisting agent for which several otherwise equivalent binding sites are available in the minicircle, the most favourable site, i.e. the site that requires the least expenditure of elastic energy, will be in a region of low intrinsic curvature for the stress-free state of DNA. Since for  $n = 1, 11, 21, 31, 41$ ,  $\Psi(\alpha)$  has its maximum at  $\alpha = 0$ , i.e. when the untwisting agent is absent, the binding of the agent results in a net decrease in the total elastic energy  $\Psi$ . Thus, we here have an example of a case in which the affinity of an untwisting (or twisting) agent for binding to a minicircle formed from DNA with an appropriate distribution of intrinsic curvature

† In our figures we show graphs of  $\Psi$  versus  $\alpha$  (with  $-360^\circ < \alpha < 360^\circ$ ) only for a range of  $\alpha$  in which the minimum elastic energy configuration is contact free under the assumption that the effective cross-sectional diameter is 20 Å. Thus, for  $S^c$  (with  $n = 1$ ) the graph of  $\Psi$  versus  $\alpha$  is presented for  $-275^\circ < \alpha < 360^\circ$ .

can be greater than its affinity for binding to an unconstrained segment with the same base-pair sequence. The graph of  $\Psi$  versus  $\alpha$  for minicircle  $S^c$  tells us that the presence of roll–twist coupling can further heighten an affinity of untwisting agents for intrinsically curved segments subject to suitable constraints.

The lack of convexity and the presence of local minima in the graphs of  $\Psi$  against  $\alpha$  for minicircles  $S$  and  $S^c$  implies that the equilibrium topoisomer distributions for those minicircles will be bimodal. The concepts of effective bending and twisting moduli and effective helical repeat do not appear useful for  $S$  and  $S^c$ .

Selected minimum energy configurations of minicircle  $S$  subject to untwisting at steps  $n = 1$  and 41 and minicircle  $S^c$  subject to untwisting at step  $n = 1$  are shown in figure 6. For comparison, that figure contains minimum energy configurations of a DNA o-ring (with stress-free circular configuration) calculated in our earlier study (Coleman *et al.* 2003); it contains 15 i units and 15 r units arranged in the sequence  $(i_5r_5)_{15}$  and is here called minicircle  $O$ .

### Nomenclature

|  |  |
|--|--|
| $A$  | bending modulus  |
| $A^{\text{eff}}$   | effective bending modulus of the DNA in an intrinsically homogeneous minicircle                  |
| $\mathcal{B}^n$  | rectangle used to represent base pair $n$  |
| bp   | base pairs   |
| $\mathcal{C}$  | polygonal curve of the $N$ line segments connecting the centres of successive base pairs         |
| $C^{\text{eff}}$   | effective twisting modulus of the DNA in an intrinsically homogeneous minicircle                 |
| $\mathbf{d}_1^n, \mathbf{d}_2^n, \mathbf{d}_3^n$                   | orthonormal basis embedded in base pair $n$  |
| $\bar{\mathbf{d}}_1^n, \bar{\mathbf{d}}_2^n, \bar{\mathbf{d}}_3^n$ | orthonormal mid-basis for base-pair step $n$   |
| $D_{ij}^n$   | components of the transformation matrix relating bases $\mathbf{d}_i^n$ and $\mathbf{d}_j^{n+1}$ |
| $F_{ij}^n$   | elastic moduli for the changes in angular variables at base-pair step $n$                        |
| $G_{ij}^n$   | elastic moduli coupling changes in angular and translational variables at base-pair step $n$     |
| $H_{ij}^n$   | elastic moduli for changes in translational variables at base-pair step $n$                      |
| $\mathbf{f}^n$   | force that $(n + 1)$ th base pair exerts on $n$ th base pair                                     |
| $f_i^n$  | components of $\mathbf{f}^n$ with respect to the basis $\mathbf{d}_i^n$                          |
| $\mathbf{m}^n$   | moment that $(n + 1)$ th base pair exerts on $n$ th base pair                                    |
| $m_i^n$  | components of $\mathbf{m}^n$   |
| $N$  | number of base pairs   |
| $\mathbf{r}^n$   | vector from the centre of the $n$ th base pair to the centre of the $(n + 1)$ th base pair       |
| $r_1^n, r_2^n, r_3^n$  | components of $\mathbf{r}^n$   |
| $\mathbf{x}^n$   | location of the centre of the rectangle used to represent base pair $n$                          |

|  |   |
|--|---|
| $\alpha$   | reduction in intrinsic twist imposed at a single base-pair step                       |
| $\gamma^n$   | direction of bending between base pairs $n$ and $n + 1$                               |
| $\eta^n, \zeta^n, \kappa^n$                            | angles employed in the definition $\theta_i^n$  |
| $\theta_1^n, \theta_2^n, \theta_3^n$                   | tilt, roll, and twist of base-pair step $n$   |
| $\bar{\theta}_1^n, \bar{\theta}_2^n, \bar{\theta}_3^n$ | tilt, roll, and twist of base-pair step $n$ in its stress-free state                  |
| $\rho_1^n, \rho_2^n, \rho_3^n$                         | shift, slide, and rise of base-pair step $n$  |
| $\bar{\rho}_1^n, \bar{\rho}_2^n, \bar{\rho}_3^n$       | shift, slide, and rise of base-pair step $n$ in its stress-free state                 |
| $\psi^n$   | elastic energy of base-pair step $n$  |
| $\Psi$   | total elastic energy of a DNA segment   |
| $\omega$   | helical twist angle   |
| $\Lambda$  | helical repeat length   |
| $\Lambda^{\text{eff}}$                                 | effective helical repeat length of the DNA in an intrinsically homogeneous minicircle |

This research was supported by the US Public Health Service under grant GM34809 and the National Science Foundation under grant DMS-02-02668.

## References

- Bauer, W. R., Lund, R. A. & White, J. H. 1993 Twist and writhe of a DNA loop containing intrinsic bends. *Proc. Natl Acad. Sci. USA* **90**, 833–837.
- Berman, H. M. & Olson, W. K. 2003 The many twists of DNA. In *DNA50: the secret of life* (ed. M. Balaban), pp. 104–122. London: Faircount LLC.
- Berman, H. M., Olson, W. K., Beveridge, D. L., Westbrook, J., Gelbin, A., Demeny, T., Hsieh, S.-H., Srinivasan, A. R. & Schneider, B. 1992 The Nucleic Acid Database: a comprehensive relational database of three-dimensional structures of nucleic acids. *Biophys. J.* **63**, 751–759.
- Brukner, I., Sanchez, R., Suck, D. & Pongor, S. 1995 Trinucleotide models for DNA bending propensity: comparison of models based on DNaseI digestion and nucleosome packaging data. *J. Biomol. Struct. Dynam.* **13**, 309–317.
- Charitat, T. & Fourcade, B. 1998 Metastability of a circular o-ring due to intrinsic curvature. *Eur. Phys. J. B* **1**, 333–336.
- Coleman, B. D. & Swigon, D. 2000 Supercoiled configurations with self-contact in the theory of the elastic rod model for DNA plasmids. *J. Elasticity* **60**, 171–221.
- Coleman, B. D. & Swigon, D. 2004 Theory of self-contact in Kirchhoff rods with applications to supercoiling of knotted and unknotted DNA plasmids. *Phil. Trans. R. Soc. Lond. A* **361**, 1281–1299.
- Coleman, B. D., Dill, E. H., Lembo, M., Lu, Z. & Tobias, I. 1993 On the dynamics of rods in the theory of Kirchhoff and Clebsch. *Arch. Ration. Mech. Analysis* **121**, 339–359.
- Coleman, B. D., Swigon, D. & Tobias, I. 2000 Elastic stability of DNA configurations. II. Supercoiling of miniplasmids. *Phys. Rev. E* **61**, 759–770.
- Coleman, B. D., Olson, W. K. & Swigon, D. 2003 Theory of sequence-dependent DNA elasticity. *J. Chem. Phys.* **118**, 7127–7140.
- Crothers, D. M., Drak, J., Kahn, J. D. & Levene, S. D. 1992 DNA bending, flexibility, and helical repeat by cyclization kinetics. *Meth. Enzymol.* **212**, 3–29.
- Dickerson, R. E. (and 16 others) 1989 Definitions and nomenclature of nucleic acid structure parameters. *J. Mol. Biol.* **208**, 787–791.

- Dill, E. H. 1992 Kirchhoff's theory of rods. *Arch. Hist. Exact Sci.* **44**, 1–23.
- Domokos, G. 1995 A group theoretic approach to the geometry of elastic rings. *J. Nonlinear Sci.* **5**, 453–478.
- Domokos, G. & Healey, T. J. 2001 Hidden symmetry of global solutions in twisted elastic rings. *J. Nonlinear Sci.* **11**, 47–67.
- El Hassan, M. A. & Calladine, C. R. 1995 The assessment of the geometry of dinucleotide steps in double-helical DNA: a new local calculation scheme. *J. Mol. Biol.* **251**, 648–664.
- Furrer, P. B., Manning, R. S. & Maddocks, J. H. 2000 DNA rings with multiple energy minima. *Biophys. J.* **79**, 116–136.
- Gorin, A. A., Zhurkin, V. B. & Olson, W. K. 1995 B-DNA twisting correlates with base pair morphology. *J. Mol. Biol.* **247**, 34–48.
- Hagerman, P. J. 1992 Straightening out the bends in curved DNA. *Biochim. Biophys. Acta* **1131**, 125–132.
- Heath, P. J., Clendenning, J. B., Fujimoto, B. S. & Schurr, J. M. 1996 Effect of bending strain on the torsion elastic constant of DNA. *J. Mol. Biol.* **260**, 718–730.
- Horowitz, D. S. & Wang, J. C. 1984 Torsional rigidity of DNA and length dependence of the free energy of DNA supercoiling. *J. Mol. Biol.* **173**, 75–91.
- Katritch, V. & Vologodskii, A. 1997 The effect of intrinsic curvature on conformational properties of circular DNA. *Biophys. J.* **72**, 1070–1079.
- Lu, X.-J. & Olson, W. K. 1999 Resolving the discrepancies among nucleic acid conformational analyses. *J. Mol. Biol.* **285**, 1563–1575.
- Lu, X.-J. & Olson, W. K. 2003 3DNA: a software package for the analysis, rebuilding, and visualization of three-dimensional nucleic acid structure. *Nucleic Acids Res.* **31**, 5108–5121.
- Lu, X.-J., Babcock, M. S. & Olson, W. K. 1999 Mathematical overview of nucleic acid analysis programs. *J. Biomol. Struct. Dynam.* **16**, 833–843.
- Lu, X.-J., Shakked, Z. & Olson, W. K. 2000 A-form conformational motifs in ligand-bound DNA structures. *J. Mol. Biol.* **300**, 819–840.
- Matsumoto, A. & Olson, W. K. 2002 Sequence-dependent motions of DNA: a normal mode analysis at the base-pair level. *Biophys. J.* **83**, 22–41.
- Nadeau, J. G. & Crothers, D. M. 1989 Structural basis for DNA bending. *Proc. Natl Acad. Sci. USA* **86**, 2622–2626.
- Olson, W. K., Gorin, A. A., Lu, X.-J., Hock, L. M. & Zhurkin, V. B. 1998 DNA sequence-dependent deformability deduced from protein–DNA crystal complexes. *Proc. Natl Acad. Sci. USA* **95**, 11163–11168.
- Olson, W. K. (and 15 others) 2001 A standard reference frame for the description of nucleic acid base-pair geometry. *J. Mol. Biol.* **313**, 229–237.
- Packer, M. J., Dauncey, M. P. & Hunter, C. A. 2000 Sequence-dependent DNA structure: tetranucleotide conformational maps. *J. Mol. Biol.* **295**, 85–103.
- Trifonov, E. N. 1991 DNA in profile. *Trends Biochem. Sci.* **16**, 467–470.
- White, J. H., Lund, R. A. & Bauer, W. R. 1996 Twist, writhe, and geometry of a DNA loop containing equally spaced coplanar bends. *Biopolymers* **38**, 235–250.
- Zhurkin, V. B., Lysov, Y. P. & Ivanov, V. 1979 Anisotropic flexibility of DNA and the nucleosomal structure. *Nucleic Acids Res.* **6**, 1081–1096.